Sediment structure and physicochemical changes following tidal inundation at a large open coast managed realignment site

Dale, J., Cundy, A. B., Spencer, K. L., Carr, S. J., Croudace, I. W., Burgess, H. M. & Nash, D. J.

Original citation & hyperlink:
Dale, J, Cundy, AB, Spencer, KL, Carr, SJ, Croudace, IW, Burgess, HM & Nash, DJ 2019, 'Sediment structure and physicochemical changes following tidal inundation at a large open coast managed realignment site' Science of the Total Environment, vol. 660, pp. 1419-1432.
https://dx.doi.org/10.1016/j.scitotenv.2018.12.323

DOI 10.1016/j.scitotenv.2018.12.323
ISSN 0048-9697
ESSN 1879-1026

Publisher: Elsevier

Sediment structure and physicochemical changes following tidal inundation at a large open coast managed realignment site

Jonathan Dale[1,2*], Andrew B. Cundy[3], Kate L. Spencer[4], Simon J. Carr[4,5], Ian W. Croudace[3], Heidi M. Burgess[1] and David J. Nash[1,6]

[1]Centre for Aquatic Environments, School of Environment and Technology, University of Brighton, Brighton, BN2 4GJ, UK.

[2]School of Energy, Construction and Environment, Coventry University, Coventry CV1 5FB, UK.

[3]School of Ocean and Earth Science, University of Southampton, National Oceanography Centre (Southampton), Southampton, SO14 3ZH, UK.

[4]School of Geography, Queen Mary University of London, London, E1 4NS.

[5]Science, Natural Resources & Outdoor Studies, University of Cumbria, Rydal Road, Ambleside, Cumbria LA22 9BB, U.K.

[6]School of Geography, Archaeology and Environmental Studies, University of the Witwatersrand, Private Bag 3, Wits 2050, South Africa.

[*]**Corresponding Author:**

Jonathan Dale

School of Environment and Technology, University of Brighton, Cockcroft Building, Lewes Road, Brighton, UK, BN2 4GJ. Email: J.J.Dale@brighton.ac.uk

Published in Science of the Total Environment, Volume XXX, pp XXX, 2019.

Keywords

Managed realignment; Microtomography; Sediment Structure; Saltmarsh Geochemistry; Itrax XRF

1 Abstract

Managed realignment (MR) schemes are being implemented to compensate for the loss of intertidal saltmarsh habitats by breaching flood defences and inundating the formerly defended coastal hinterland. However, studies have shown that MR sites have lower biodiversity than anticipated, which has been linked with anoxia and poor drainage resulting from compaction and the collapse of sediment pore space caused by the site's former terrestrial land use. Despite this proposed link between biodiversity and soil structure, the evolution of the sediment sub-surface following site inundation has rarely been examined, particularly over the early stages of the terrestrial to marine or estuarine transition. This paper presents a novel combination of broad- and intensive-scale analysis of the sub-surface evolution of the Medmerry Managed Realignment Site (West Sussex, UK) in the three years following site inundation. Repeated broad-scale sediment physiochemical datasets are analysed to assess the early changes in the sediment subsurface and the preservation of the former terrestrial surface, comparing four locations of different former land uses. Additionally, for two of these locations, high-intensity 3D-computed X-ray microtomography and Itrax micro-X-ray fluorescence spectrometry analyses are presented. Results provide new data on differences in sediment properties and structure related to the former land use, indicating that increased agricultural activity leads to increased compaction and reduced porosity. The presence of anoxic conditions, indicative of poor hydrological connectivity between the terrestrial and post-inundation intertidal sediment facies, was only detected at one site. This site has experienced the highest rate of accretion over the terrestrial surface (*ca*. 7 cm over 36 months), suggesting that poor drainage is caused by the

52 interaction (or lack of) between sediment facies rather than the former land use. This has
53 significant implications for the design of future MR sites in terms of preparing sites, their
54 anticipated evolution, and the delivery of ecosystem services.

55

56

2 Introduction

Saltmarsh and mudflat environments provide a range of ecosystem services (Costanza et al., 1997) including detoxification, nursery habitat and flood defence through the attenuation of wave energy (e.g. Moller et al., 2014; Rupprecht et al., 2017). However, these habitats are threatened by sea level rise, causing erosion and coastal squeeze (e.g. Doody, 2004), and anthropogenic pressures including pollution and reclamation in response to urbanisation and population growth. This has resulted in the loss and degradation of coastal habitats worldwide. In recent years, there have been a number of schemes implemented to compensate for these losses, frequently driven by legislative requirements to improve habitats and biodiversity such as the EU Habitats Directive (European Parliament and the Council of the European Commission, 1992). These schemes use ecological engineering (or ecoengineering) approaches (Bergen et al., 2001) and aim to restore the structure and function of intertidal environments, either through habitat creation or by engineering physical processes to create the desired conditions to encourage habitat creation (Elliott et al., 2016). This paper focuses on managed realignment (MR), one of the most popular coastal ecoengineering techniques.

MR describes the practice of inundating areas of the coastal hinterland through de-embanking, removing or breaching the former flood defences, with new defences constructed inland. Yet, growing evidence suggests that saltmarshes within MR sites have lower biodiversity and abundance of key species than anticipated (e.g. Mazik et al., 2010; Mossman et al., 2012), which may have consequences for ecosystem functioning (Doherty

et al., 2011). These differences have been associated with abiotic factors such as nutrient availability, salinity and redox conditions (Erfanzadeh et al., 2010; Mossman et al., 2012). MR is often carried out in areas of former saltmarsh and mudflat habitat, which have been previously reclaimed through the construction of embankments and then drained for agriculture. As a consequence, the practice results in the restoration and re-creation of historical intertidal habitats (as opposed to creating "new" habitats). Reclamation and drainage leads to compaction, de-watering and mineralisation of organic matter, resulting in irreversible changes to the sub-surface sediment structure (including the collapse of pore space) (e.g. Crooks and Pye, 2000; Hazelden and Boorman, 2001; Spencer et al., 2017). This has led to poor drainage in many MR sites following site inundation and reduced vertical hydrological connectivity between the relict terrestrial horizon and the freshly deposited intertidal sediment (e.g. Crooks and Pye, 2000; Hazelden and Boorman, 2001; Tempest et al., 2015).

The flux of pore water through the sub-surface sediment is considered to be crucial for controlling abiotic conditions, and therefore could exert a major influence on vegetation colonisation in MR sites (Davy et al., 2011; e.g. Howe et al., 2010; Wilson et al., 2015). However, there remains a shortage of data on the evolution of sub-surface sediment geotechnical and geochemical properties following inundation at MR sites (Esteves, 2013). This is especially true for investigations into the critical period immediately following site inundation (i.e. in the early stages of the terrestrial to marine or estuarine transition) as it is these surface conditions that will form the substrate for seedling germination, with particular focus required into:

(a) the preservation of the relict terrestrial horizon, and its structural, physical and chemical characteristics, post-inundation, and

(b) the development of the sub-surface geochemical profile in response to the former terrestrial land use.

This study investigates the impact of different pre-managed realignment land use practices on the early evolution of the sub-surface sediment structure and geochemical environment at the Medmerry Managed Realignment Site (West Sussex, UK), during the first three years of site inundation (covering the early stages of the transition from a terrestrial to a marine / coastal lagoonal system). Specifically, a novel combination of broad- (centimetre to decimetre) and intensive- (micron) scale sedimentary data sets, from samples taken at two time points, are analysed to assess the differences and the early evolution of the sub-surface geochemical profile and sediment structure for sites of differing former land use. The implications of these differences for the longer term development of sediment structure, drainage and physicochemical properties, in relation to site evolution, management, and ecosystem service delivery, are discussed and assessed.

3 Study Site

The Medmerry Managed Realignment Site (Figure 1) is located within the Solent, southern UK, on the western side of the Manhood Peninsula (Figure 1, insert). Previously, the area

had been a brackish lagoon (Krawiec, 2017) behind a shingle barrier beach, which had drained through Pagham Harbour on the eastern side of the peninsula. However, this area was separated from Pagham Harbour and reclaimed through the construction of an embankment, and subsequently drained, between 1805 and 1809 (Bone, 1996). Coastal flood defence for the reclaimed area at Medmerry was provided by the shingle barrier beach, which was managed by the Environment Agency (UK). To maintain the necessary defence standard, constant work was required each winter to recycle and re-profile the shingle bank. Nevertheless, the defences remained vulnerable during storm events; the bank was breached 14 times between 1994 and 2011, flooding homes, local holiday caravan parks and agricultural land. The coastal flooding and erosion risk was reviewed in the Pagham to East Head Coastal Defence Strategy (Environment Agency, 2007), which endorsed MR as the most suitable method of managing the risk of coastal flooding.

The Medmerry scheme, which is the largest open coast MR site in Europe (at the time of site inundation), was designed not only to provide a sustainable and cost-effective method of coastal flood risk management, but also to compensate for saltmarsh and mudflat habitat loss elsewhere in the region. Over 80% of the Solent's coastline is designated for its nature conservation interest (Foster et al., 2014), yet 40% (approximately 670 hectares) of saltmarsh in the region were lost through erosion between 1971 and 2001 (Cope et al., 2008). Over the one hundred years following construction of the Medmerry site, it was estimated that up to 184 hectares of new intertidal and transitional habitat would be created (Pearce et al., 2011).

147 Construction of the site began in autumn 2011, which included 7 km of new earth “bund”
148 defences, reaching 3 km inland. Freshwater drains through the site via four drainage outlets
149 with tidal gates constructed into the new defences. The site was breached on 9th
150 September 2013 through a single narrow opening in the shingle bank, forming a semi-
151 diurnal, mesotidal, semi-enclosed, fetch and depth limited estuarine system. At the time of
152 this study, high water at the furthest point inland occurred approximately 50 minutes after
153 high water at the breach (Dale et al., 2018b). During low tide, draining water is constricted
154 to the main channels running through the site (Figure 1), which in some cases drain to near
155 emptiness. Sediment is imported, and exported, from the wider coastal environment, but
156 Dale et al. (2018b) identified that larger concentrations are currently being internally
157 redistributed as the site responds to the introduction of intertidal inundation.

158

4 Materials and Methods

Six sediment cores were taken from the Medmerry site in each of 2015 and 2016. All sampling was performed at low water. Cores 1 to 4 were collected for broad-scale analysis, Cores 5 and 6 for intensive-scale analysis. Sampling was carried out at four locations within the Medmerry site. These locations were selected based on differences in former (terrestrial) land use. Cores 1 and 5 were taken from a former area of pastoral land, occasionally used for low quality (usually unsuccessful) arable agriculture. Cores 2 and 3 were from a former area of pastoral land, with Core 2 taken from a non-vegetated surface and Core 3 from a vegetated surface. Cores 4 and 5 were from a former intensive arable field, last harvested two weeks prior to site inundation, behind an area of lower elevation land which has experienced rapid accretion of coarse grained sandy sediment (d_{50} = 47.33 ± 0.91 µm) following site inundation (Dale et al., 2017). The expected differences in sediment structure as a result of the former land use are outlined in Table 1. The presence and extent of these proposed differences were assessed initially on a broad centimetre scale, followed by analysis carried out on an intensive (micron) scale.

4.1 Sampling and Methods for Broad (centimetre to decimetre)-Scale Analysis

Vertical sediment cores were taken in January 2015, 16 months after the site was breached, and September 2016, 36 months after site inundation, to evaluate differences in the sediment sub-surface physical properties and geochemistry. Two cores were taken in

parallel, at approximately the same elevation (± 2 cm) and within 30 cm of each other, at each sampling location using a hand driven large (5cm diameter, stainless steel) gouge corer, transferred to open PVC tubes and wrapped in PVC film. Due to topographic variations within the site it was not possible to sample at identical elevations at the four sampling sites, but all sites were approximately in the same position in the intertidal zone and therefore are expected to have similar hydroperiod conditions. Core depths varied between 26 and 49 cm, although parallel cores were not always taken to the same depth. Sediment cores were collected at least 15 m from the channel to minimise the influence of lateral sub-surface flow (Marani et al., 2006).

Samples were stored at + 3.6 °C until analysis. Sediment properties were visually described and one core from each site was subsampled at 1 cm depth increments. Following hydrogen peroxide treatment and dispersion with sodium hexametaphosphate, a Malvern Instruments Mastersizer Hydro 2000G Laser Diffraction Particle Size Analyser was used to determine the grain size distribution in sediment subsamples. Subsamples were also examined for a suite of elements using an Inductively Coupled Plasma-Optical Emission Spectrometer (ICP-OES). Samples were digested with Aqua Regia (modified from Berrow and Stein, 1983). Aqua Regia was prepared with a 30% HNO_3 : 70% HCL (1:3) mixture at room temperature. 0.1 ± 0.01 g of sample, oven dried at 105 °C, was digested in 3 ml of Aqua Regia for three hours in a water bath at 80 °C. Following digestion, 7 ml of distilled water were then added to the sample. A 1:10 dilution of the solution was made with distilled water for analysis using a Perkin Elmer Optima 2100 DV ICP-OES. To assess the elemental recovery of the digestion procedure the measured values were compared to the

quoted values for a Certified Reference Material (CRM) digested and analysed alongside the samples (e.g. Cochran et al., 1998). The Mess-4 Marine Sediment (National Research Council Canada) CRM was used and recovery values were generally within ± 25% of the reported values (see supporting information). Process blanks and repeat samples were analysed every 20 samples for quality control and analytical error. Process blanks were below detection limits and repeat samples were within ±10 % throughout.

For the remaining cores, a known quantity of sediment was extracted using a syringe at 1 cm intervals and analysed for wet bulk density, moisture content, porosity and loss on ignition (a proxy for organic content). The moisture content was measured as a percentage of the dry mass (moisture content = water weight / dry sediment weight x 100) after samples had been oven dried at 105 °C for 48 hours. Porosity was calculated using the dry bulk density, assuming a particle density of 2.65 g cm^{-3} as stated by (Rowell, 1994) based on typical data. The organic content of the samples was estimated via the loss on ignition proxy method, following ignition of subsamples for six hours at 450 °C.

4.2 Sampling and Methods for Intensive (micron)-Scale Analysis

Smaller sediment cores were recovered from the same coring locations as Core 1 and Core 4, labelled Cores 5 and 6 respectively, in July 2015 and September 2016. These sites were selected to analyse the influence that different intensities of arable agricultural activity have on the subsurface sediment structure (i.e. by using sites with / without a history of intensive

arable agriculture). Cores were taken from within 2 m of the broad-scale coring sites, using the advanced trimming method (Hvorslev, 1949). 44 mm diameter clear PVC tubes were inserted into the sediment, trimming the surrounding sediment to minimise the disturbance to the sample. Core lengths varied between 7.9 cm and 11.1 cm. The ends of the sample tubes were capped and wrapped in PVC film secured with tape to prevent moisture loss. Cores were kept upright during transport and storage to minimise any disturbance and, on return to the laboratory, were stored between + 3.6 °C and + 4 °C.

3D-computed X-ray microtomography (µCT) is a non-destructive imaging method that has been successfully applied to the study of saltmarsh sediment structure (Cnudde and Boone, 2013; Ketcham and Carlson, 2001; Spencer et al., 2017). µCT analysis was carried out here to identify the sediment bulk phases and stratigraphy (for an assessment of the comparability of the broad- and intensive-scale methodologies) and to analyse the key structural and stratigraphic differences (total porosity, characterisation of the pore networks) between the two sampled sites, at a much higher resolution than the broad-scale approach described above. Whilst only single core samples were analysed in both years per core site, previous analysis of this type (e.g. Spencer et al., 2017) has recognised that single core samples may be used as a representation of the sediment structural characteristics. Sealed core tubes were scanned at 76 µm resolution using a Nikon Metrology XT H 225 X-ray CT system with Perkin Elmer XRD 0820 CN3 16-bit flat panel detector at Queen Mary, University of London. Inspect-X was used to perform the scans and X-radiogram acquisition and reconstruction was undertaken in CTPro. Drishti 2.1 volume rendering software was used for visualisation of the reconstructed 3D models to identify bulk phases and inform segmentation following

249 the method of Spencer et al. (2017). Each 3D volume was sub-sampled further into four
250 equally sized depth increments, labelled A (base) to D (top), for detailed quantification of
251 differences in porosity with depth.

252

253 Cores were split vertically, photographed and analysed using Itrax non-destructive micro-X-
254 ray fluorescence spectrometry analysis (Croudace et al., 2006) for a range of elemental data
255 to compare changes in geochemistry with sediment structure analysis provided by the μCT,
256 at a 200 micrometre scale which was not possible using ICP-OES analysis. The Itrax produces
257 elemental data in counts but previous studies (e.g. Miller et al., 2014) have shown that
258 these data correlate well with quantitative analytical data (e.g., ICP-OES or Wavelength
259 Dispersive X-ray Fluorescence). Furthermore, the high frequency compositional changes
260 identified using the Itrax are often missed when analysing lower resolution bulk sub-
261 samples using more traditional, destructive, analytical methods. Each core was loaded onto
262 a horizontal cradle and scanned at a resolution of 200 μm at the BOSCORF laboratories,
263 National Oceanography Centre (Southampton). Cores were scanned wet to preserve
264 internal structure, with the software correcting for water content. Core Scanner Navigator
265 software was used to control the scanner, and data were plotted and displayed using Q-
266 Spec software. The Itrax scanner combines an X-ray line camera with a narrow, parallel,
267 high-flux X-ray beam to record a radiograph at 55 kV. XRF analysis was performed at 30 kV
268 (using a Mo anode X-ray tube, counting time 30s). Data were plotted using ItraX-Plot,
269 described by Croudace et al. (2006).

270

5 Results

5.1 Broad-scale (centimetre to decimetre) Physicochemical Changes in the Subsurface (Cores 1 to 4, 2015 and 2016)

Sediment cores 1 to 4 exhibited clear vertical zonation and could be divided into three facies (from core base to core surface) based on the environmental and land use change known to have occurred at the Medmerry site; (i) a pre-reclamation intertidal unit (*Unit A*), (ii) a reclamation boundary and soil unit formed since site reclamation between 1810 and 1880 (*Unit B*), and (iii) a terrestrial boundary and post-breach intertidal unit dating from site inundation in September 2013 (*Unit C*). The depth, composition and structure of the three units varied between sites.

5.1.1 Physical Characteristics

Average physical sediment characteristics for the three units are presented in Table 2 (see supplementary material for core descriptions and full datasets). Wet bulk density ranged from 0.64 to 2.18 kg m^{-3} and tended to increase with depth. Both moisture content (36.62 – 123.08 %) and porosity (0.33 – 0.81) decreased with depth, whereas loss on ignition values varied from 3.24% to 19.21% and fluctuated through the sample. Coarser grained sediments were generally found in the Unit A, compared to Units B and C, except in Core 4 where coarser grained sediments (d_{50} = 67.87 (2015) and 49.77 (2016)) were found at the sediment

surface. Median grain sizes ranged from 5.46 to 46.48 µm, and the mud content (clay + silt) varied between 54.1 and 97.67 %. Statistical differences between sediment units were assessed via a Kruskal Wallis test ($n = 22$ to 45, $p < 0.05$) for the whole dataset with the exception of Core 4_{16} as no vertical zonation was found in this sample. Statistical differences were found between the three sediment units for all parameters except for particle size analysis (median grain size and mud content).

5.1.2 Geochemical Profiles

ICP-OES-derived major element data (Al, Ca, Fe, Mn, S, Na) are presented for 2015 (Figure 2) and 2016 samples (Figure 3). To account for variations in sediment composition, data have been normalised to Al (after Spencer et al., 2008). Ca decreased with depth through Unit C in all 2015 samples and Cores 2 and 3 in 2016. This may be the result of decalcification, typical of oxic saltmarsh sediments as a result of a lowering of the pH caused by nitrification and decomposition of organic matter (Luther and Church, 1988; Vranken et al., 1990), and then re-precipitation at depth. However, the scale of the decrease, and subsequent increase in Unit A (Core 1_{15} and Core 4_{15}) could also be indicative of the presence of finely comminuted shell debris in the intertidal sediments (Units A and C).

The diagenetic cycles of Fe and Mn have been well documented for saltmarsh sediments (e.g. Spencer et al., 2003; Zwolsman et al., 1993). A peak in Fe or Mn concentration may indicate redox mobilisation and reprecipitation, whereas an increase in S may represent

315 bacterially-mediated reduction of sulphate and formation of early-diagenetic sulphide
316 minerals (Cundy and Croudace, 1995). In both years at coring locations 1, 2 and 4, and in
317 Core 3_{15}, Fe and Mn concentrations were relatively homogenous down core with some
318 variability within Unit B, potentially caused by residual Fe concretions from the legacy of
319 ploughing within this zone, without any consistent or clear peaks. This is suggestive of a
320 fluctuating water table through the sediment sub-surface, consistent with the visual
321 observations of Fe-stained mottled sediment in this zone (see supplementary material); this
322 may be the result of tidal variability causing changes in the redox boundary, preventing the
323 formation of a stable redox zone and a strong Fe and Mn peak (Cundy and Croudace, 1995;
324 Zwolsman et al., 1993). However, in Core 3_{16}, Fe fluctuated throughout the depths
325 examined, peaking in the middle terrestrial zone. A clearer trend was observed in the
326 concentration of Mn, which is more sensitive than Fe to changes in redox status, with Mn
327 peaking at the boundary between the post-breach intertidal and terrestrial facies suggesting
328 possible diagenetic enrichment of Mn. S concentration decreased with depth, matching the
329 changes in Na concentration, and therefore implying that variations in S are driven primarily
330 by the introduction and evaporation of sea water.

331

332 Principal component analysis (PCA) was performed on the entire dataset to differentiate
333 between the physical and geochemical characteristics of the different units. PCA is a data
334 reduction technique which calculates new variables, or principal components, from linear
335 combinations of the original parameters and has been used successfully elsewhere to
336 (partially) discriminate geochemical data in coastal sediments (e.g. Cundy et al., 2006). The
337 first principal component accounts for the greatest variability, with every subsequent

component accounting for less of the variability (Reid and Spencer, 2009). Therefore, PCA allows for grouping of different depths based on their physicochemical variability. Results reveal clear differences between the PCA scores for Units A and C (Figure 4). Unit B also demonstrated some evidence of grouping, but overlapped the other two units.

5.2 Intensive-scale (micron) Subsurface Structure Physicochemical Characteristics

5.2.1 Sediment Structure

Representative µCT reconstructions of sediment structure, with a voxel size of 65 µm, are presented for coring locations 5 (taken from an area of former lower intensity arable agriculture) and 6 (an area of former high intensity arable agriculture) in Figure 5. Core 5 demonstrated a relatively consistent solid matrix phase (Figure 5a) in both years sampled, with no separate sediment facies, suggesting there has been no (or very minimal) post-site inundation deposition of sediment. This is despite the broad-scale geophysical analysis suggesting that a small, 2 cm, new intertidal sediment unit was present. It is, therefore, possible that these different units might be present, but that they are sufficiently similar in sediment structure to be indistinguishable via µCT analysis. In contrast, structural differences were clearly visible in Core 6_{15} (Figure 5b). Laminations were present in a compact upper sediment facies, consisting of sandy sediment deposited following site inundation, overlying the former terrestrial soil that had been used intensively for arable agriculture up to two weeks prior to site inundation. A sharp, irregular boundary occurred between the two units and is marked on Figure 5b. No evidence of the upper sediment

361 facies was found in the Core 6_{16} sample (Figure 5b), probably due to the local remobilisation
362 of sediment in response to observed changes in the site's hydrodynamics, and
363 morphological evolution in response to the introduction to intertidal inundation (Dale et al.,
364 2018a).

365

366 Macroporosity (pores > 80 μm; Beven and Germann, 2013) measurements and
367 characteristics are presented in Table 3, and plotted for each of the four sub-samples in
368 Figure 6. In Core 5_{15}, a large, interconnected, pore space was detected through the sample,
369 whereas the Core 5_{16} pore structure consisted of horizontal elongated macropore networks.
370 In Core 6_{15}, a sheet like macro-pore was detected across the division between the units,
371 although it is likely that this an artificial feature caused by the coring process (which
372 resulted in sediment cracking along this interface), with a large horizontal macropore
373 dominating the lower facies. There was also no evidence of this horizontal pore system in
374 Core 6_{16}, with the macropore network dominated by a vertical pore (on the left of the 2016
375 macro-pore phase in Figure 5b) and areas of isolated, flattened pore space.

376

377 Bulk macroporosity in Core 5 was generally moderate to high (5.6 – 22.4 %) and decreased
378 with depth (Figure 6), as would be expected due to sediment compaction effects. Less
379 variability was observed in Core 6, where bulk macroposity was low to moderate (3.5 – 13.1
380 %). The degree of pore connectivity is indicated by the Euler-Poincaré characteristic, a
381 measure of the number of redundant connections within the pore network expressed as a
382 function of the volume, with decreased connectivity indicated by increased positive values,

and increased connectivity demonstrated by decreased negative values (Vogel, 1997). All samples followed a trend of decreasing connectivity upwards, and then increasing in the upper sub-sample, reflecting an increase in redundant connections and more tortuous pore networks in the upper and lower sediment sub-sections. Connectivity was greater in 2015 compared to 2016 at both sites and was greater in Core 5 compared to Core 6, suggesting greater levels of compaction due to higher levels of agricultural activity and an increase in compaction at both sites as each evolved following site inundation.

The mean number of branches per pore were calculated through the transformation of macropores into topological networks of nodes and branches, and used as an indication of pore network complexity (Polder et al., 2010). Pore networks were more complex in Core 6 than Core 5, but at both sites decreased in complexity between 2015 and 2016. This suggests that pore system complexity decreases over time following site inundation, due to either the hydraulic head of tidal water above the sediment causing compaction or sediment being flushed out as the water drains causing the pore networks to collapse (Dale et al., 2018a). No distinct pattern was present in the Core 5_{15}, but in Core 5_{16} the upper sub-sample had a greater number of branches per pore compared to the rest of the sample. In contrast, complexity in Core 6 decreased upwards, but increased in the upper sub-section consisting of the post-breach sediment facies. The degree of anisotropy is representative of similarity in arrangement and the directness of the branches of the dominant macropore system (Odgaard, 1997). In 2015, pores were more aligned in Core 5 than Core 6, although anisotropy was much lower in the basal sub-samples of Core 5 (A and B). Anisotropy was higher in the post-breach sediment facies in Core 6_{15}. In comparison, macropores

406 demonstrated a similar level of organisation in Core 5_{16}, whereas Core 6_{16} had a higher
407 anisotropy value representing an increase in similarity in the arrangement of the pore
408 networks.

409

410 **5.2.2 Sediment Geochemistry**

411

412 Itrax scanning was employed to examine the variability of nine elements at high spatial
413 resolution (200 µm). The content of coarse grained sediment, indicated by the Zr and Cr
414 intensity (which are frequently associated with heavy mineral assemblages in detrital sands,
415 e.g. Cundy et al., 2006), remained relatively constant in Core 5_{15} (Figure 7a). Two major
416 peaks were observed in the Cr intensity, although the second of these peaks corresponded
417 with an area of high intensity present on the radiograph likely to be a clast. Measurements
418 of the K intensity indicate that the fine grained fraction decreased in the middle section of
419 the sample, increasing again deeper in the sample, which is also reflected in Si and the bulk
420 µCT attenuation measurements (Figure 5a). Similar trends were observed in the Cl and Ca
421 intensity. Black sediment, low Fe and Mn, and a peak in S, suggest possible bacterial
422 reduction of sulphate within the cracked and desiccated near-surface sediments (Figure 5a),
423 although broadly coincident peaks in Cl and Ca may indicate that the peak in S is at least
424 partly a function of increased porewater sulphate rather than sulphate reduction processes.
425 Fe and Mn increased below this unit and remained constant throughout the rest of the
426 sample, with three relatively large peaks. However, the Fe peaks corresponded with peaks
427 in X-ray intensity (kcps) and are likely to be the product of X-ray response rather than

428 increases in concentration. After peaking in the near-surface sediment, S followed a similar
429 pattern to Si, K, Cl and Ca.

430

431 No major vertical changes in bulk sediment composition were detected in Core 5_{16} (Figure
432 7b), demonstrated by the relatively constant distribution of Si with the major peaks
433 corresponding to variability in the X-ray response (kcps). These observations were
434 supported by similar trends in Zr and Cr intensities, although peaks were also observed in
435 these elements corresponding to the presence of high density material (clasts, evident in
436 the X-radiograph image). The distribution of K indicated relatively constant clay content
437 within the sample. Cl decreased slightly down-sample, whereas Ca decreased in the lower
438 section of the sample, indicative of decalcification. In contrast to the other elements, Mn
439 showed a strong increase in intensity in the middle part of the core, possibly reflecting early
440 diagenetic enrichment, although this observation was not supported by change in the Fe
441 intensity. However, analysis of the Fe / Mn ratio (Figure 8) indicated higher concentrations
442 of Mn to Fe in the middle of the core, suggesting mildly reducing conditions and early
443 diagenetic mobilisation of Mn. No evidence of the bacterial reduction of sulphate, possibly
444 present in the near-surface of the previous sample, was found, and trends in S generally
445 coincided with peaks in Cl and Ca so may be caused by increased porewater sulphate rather
446 than microbially-mediated sulphate reduction.

447

448 Coarse grained sediments dominated the near-surface component of Core 6_{16} (Figure 7c),
449 visible in the photographic image and indicated by the high intensity of Zr. Several peaks in

450 Cr were detected in the upper part of the core, likely to correspond to the laminations
451 observed in the µCT scan (Figure 5b). At the boundary between the post-breach and
452 terrestrial sediment facies Cr peaked below a unit of low density detected by the
453 radiograph, matching the sheet-like pore space present in the µCT scan (Figure 5b). Below
454 this unconformity, K intensity increased, and Zr / Cr decreased, indicating an increase in fine
455 grained sediment. Cl generally decreased through the sample, whereas Ca decreased and
456 then increased again. Evidence of sub-surface diagenetic enrichment of Mn was provided by
457 an increase, and peak, in intensity in the lower third of the core. The peak in Mn
458 corresponded to an area of low density measured by the radiograph, although this is not
459 visible on the photography. It is possible that this area is the large horizontal macro-pore
460 feature present in the µCT analysis. The concentration of Fe also increased through the
461 sample, with areas of enrichment corresponding to red mottling on the sample. The Fe / Mn
462 ratio decreased through the upper 2 cm of the sample (Figure 8), but increased again at a
463 similar depth to the large horizontal macro-pore. Below the terrestrial boundary, S intensity
464 decreased through the sample. Small scale increases in S intensity occurred in areas where
465 red mottling of the sediment was not present.

466

467 In Core 6_{16} (Figure 7d) coarser grained sediments were only found in the surface sediment,
468 indicated by the surface peak in Zr, consistent with the findings from the broad-scale and
469 µCT analysis. Trends in K suggested increased clay content was present in the middle of the
470 sample. A peak in Cl occurred within the upper sub-surface, corresponding to a peak in S,
471 which could indicate the depth of saline intrusion into the sediment. Fe and Mn decreased
472 through the top of the red mottled surface sediment. Fe, and to a lesser extent Mn,

473 increased through the middle of the sample, supporting visual observations of red mottling,

474 with an additional increase present in the deeper parts of the sample.

475

6 Discussion

6.1 Preservation of the Pre-Breach Terrestrial Surface

Observations made at other, older, MR sites suggest that visual changes in the sediment characteristics associated with a terrestrial boundary or horizon would no longer be present after a number of years. For example, no visual evidence of a terrestrial facies was found at Orplands Farm Managed Realignment Site 8 years after site inundation (Spencer et al., 2008), although at this site a terrestrial horizon could still be detected through analysis of physicochemical properties of the sediment. Broad-scale analysis from four locations at the Medmerry Managed Realignment Site provided visual evidence that a sub-surface unconformity could still be detected at all sites except for Core 4_{16}, the nearest site to the breach (in a significantly higher energy environment than the other sites sampled). However, no uniform stratigraphic marker of the terrestrial surface such as the organic rich peaty horizon identified at Pagham Harbour by Cundy et al. (2002) or the alternating peat-mud (i.e. terrestrial – marine) couplets used elsewhere as indicators of tectonic activity and sea level change in coastal and near-coastal sediments (e.g. Shennan et al., 1996; Shennan et al., 1998) was found, although these have been suggested to be inconsistently preserved in some suddenly submerged intertidal environments (Cundy et al., 2000). In each sample where a sub-surface unconformity was detected, a lower pre-reclamation sediment facies was also detected. PCA allowed (partial) discrimination of samples based on combined physical and geochemical sediment properties, as opposed to a single indicator such as loss

498 on ignition or changes in particle size, into groups which corresponded to one of the three
499 vertical sediment facies; post-breach, terrestrial or pre-reclamation sediments.

500

501 The reclamation of saltmarshes results in modification to sediment structure and properties
502 (e.g. Crooks et al., 2002; Hazelden and Boorman, 2001) as a result of de-watering and
503 organic matter mineralisation, decreasing the porosity and increasing the bulk density. After
504 the re-introduction of intertidal conditions through MR, the legacy of these changes can still
505 be detected, with low moisture contents still being found at depth several decades after site
506 inundation (Spencer et al., 2017). Analysis of sites of different former land use at Medmerry,
507 16 months after site inundation, indicated similar bulk densities and porosities within the
508 terrestrial facies regardless of former site activity and land use. However, moisture content
509 and loss on ignition were higher in Cores 2 and 3, areas which previously had not been
510 subjected to arable agricultural practices (i.e. ploughing).

511

512 Detailed examination of the 3D sediment structure through the use of µCT allowed
513 comparisons of the morphology and connectivity of the sediment macro-porosity at
514 different coring locations to be made. In Core 5, taken from a site that was previously used
515 occasionally (and usually unsuccessfully) for agriculture, no new intertidal sediment unit was
516 detected despite evidence of separate units in the broad-scale analysis. It is possible that
517 differences observed in the broad-scale analysis are the result of the terrestrial unit
518 transitioning into an intertidal sedimentary environment, rather than consisting of sediment
519 deposited following site inundation. This is reflected in the similarity in the matrix of the

520 sediment detected by the μCT analysis and the gradual transition between the units
521 observed in Core 1_{16}. Core 5 had a greater bulk macroporosity throughout the sediment
522 sub-surface, with simpler pore networks that were more connected and had greater
523 similarity in arrangement than Core 6, which had been used consistently for high intensity
524 agricultural activity. This indicates that, as a result of the legacy of different terrestrial
525 agriculture practices, different sub-surface structures exist in terms of sediment
526 macroporosity, which is likely to affect the drainage characteristics and therefore
527 geochemical profiles within the sediment subsurface. Terrestrial and post-breach facies
528 were detected in the 2015 3D sediment structural analysis performed on Core 6. The top
529 facies consisted of laminated sediment deposits, which had accreted post-site inundation.
530 When re-sampled, only one sediment facies was detected. This is potentially the result of
531 local remobilisation of intertidal sediment deposited post-site inundation, likely to be in
532 response to changes in site hydrodynamics and morphological evolution as the realignment
533 site evolves.

534

535 Analysis of physical characteristics and structure of the sediment at Medmerry indicate
536 differences in sediment composition, properties and macroporosity for sites of differing
537 former land use, with the terrestrial soil unit still detectable visibly at some sites up to three
538 years after site inundation. These differences may well have consequences for the
539 development of geochemical profiles, which might limit the colonisation of saltmarsh
540 vegetation (Davy et al., 2011) and explain the lower biodiversity and abundance of key
541 species observed elsewhere (e.g. Mazik et al., 2010; Mossman et al., 2012). Importantly,
542 however, levels of sediment accretion over the terrestrial unit were much lower than at

other older sites (typically 20 to 40 mm at Medmerry compared to, for example, *ca.* 60 mm at Orplands Farm) (Spencer et al., 2008), which may partly mitigate any discontinuities in hydrological connectivity caused by the deposition of intertidal sediment on top of the preserved terrestrial surface.

6.2 Implications for Geochemical Profile Development at Managed Realignment sites

Typical vertical saltmarsh geochemical profiles are controlled by strong physicochemical gradients in pH and redox potential, and microbially-mediated organic matter breakdown using electron acceptors such as O_2, MnO_2 and $Fe(OH)_3$ (e.g. Koretsky et al., 2005; Spencer et al., 2003). Following reclamation and ploughing large-scale precipitation of Fe oxyhydroxides and other Fe-rich minerals would be anticipated (Auxtero et al., 1991; Violante et al., 2003). When re-introduced to intertidal conditions remobilisation of Fe by the saline water is expected through dissimilatory reduction of sulphate or dissolved Fe being re-distributed by advection caused by the local hydrology (Burton et al., 2011; Johnston et al., 2011). However, impeded vertical solute and porewater transport caused by the presence of an aquaclude-like boundary in the sediment sub-surface (e.g. Tempest et al., 2015) may result in inadequate drainage, stagnant porewater and a lack of aeration. The occurrence of these conditions will inevitably prevent the formation of suitable oxic conditions for re-precipitation of Fe, and Mn, at the sediment surface (Spencer et al., 2008).

No evidence of an aquaclude was found in either of Cores 2 and 3. In Core 2_{15}, Fe peaked at the terrestrial boundary, corresponding to a peak in loss on ignition values. The increase in residual bulk organic matter, present on the terrestrial surface before site inundation, may well drive bacterially-mediated sulphate reduction following incorporation into the sediment, resulting in the enrichment of Fe via Fe-sulphide formation. No major trends were detected in Fe content through the rest of the sample, where the sediment showed clear red mottling, implying variability in the water table caused by tidal inundation (Cundy and Croudace, 1995). Fe fluctuated through the red mottled Core 3_{15}, indicating a fluctuating water column through the sub-surface sediment.

Core 2_{16} was visibly darker in the intertidal and terrestrial facies, decreasing in S and increasing in Fe and Mn to the boundary between the units. The sharp nature of this boundary, and the peak in moisture content may indicate reduced vertical conveyance of water through the unconformity. The fluctuations in Fe, and to a lesser extent Mn, in the pre-reclamation intertidal facies could be caused by trapping authigenic carbonate / sulphide formation (Cundy and Croudace, 1995). In Core 3_{16}, the distribution of Fe continued to indicate a fluctuating water column.

Broad- and intensive-scale analysis suggests evidence of bacterial reduction of sulphate at the surface of Core 1_{15} and Core 5_{15}. Below this unit the red mottled sediment and Fe profile implied a variable water column facilitated by the extensive inter-connected macro-pore network indicated by µCT analysis. An increase in the Fe / Mn ratio in the middle of the

587 sample analysed using high resolution Itrax scanning in Core 5_{16} suggests redox mobilisation
588 of Mn, which is generally more sensitive to redox changes than Fe. Despite the differences
589 in sediment structure between Core 5 and 6, there was still evidence of Fe enrichment. The
590 macro-pore network was dominated by a large horizontal pore which corresponded to an
591 increase in the intensity of Mn and the Fe / Mn ratio in Itrax data, possibly the result of
592 enrichment via lateral through-flow and indicative that the pore was not an artificial by-
593 product of the sampling procedure. These trends were maintained when re-sampled with
594 no sub-surface unconformity detected in Core 6_{16}. Results presented here differ from the
595 geochemical and redox profiles observed in older MR sites (Spencer et al., 2008), and
596 natural saltmarsh and mudflat environments within the Solent (e.g. Cundy and Croudace,
597 1995). It remains to be seen if the geochemical profiles evolve in a similar manner to other
598 MR sites or towards that of a more typical intertidal setting, compared schematically in the
599 Graphical Abstract, and the timescales required for this development. Not only would this
600 determine the depth of any anoxic layer, which may inhibit biological activity, but will
601 influence nutrient exchange and the partitioning (and possibly release) of contaminants
602 such as metals or pesticides potentially stored within the sediment.

603

604 **6.3 Influence of the Former Land Use and Site Construction**

605

606 MR aims to restore the structure and functioning of intertidal habitats, compensating for
607 losses elsewhere. However, previous studies have demonstrated differences in the physical,
608 geochemical and hydrological characteristics of saltmarshes in MR sites, particularly at the
609 Orplands Farm site (UK), compared to natural marshes (Spencer et al., 2017; Spencer et al.,

2008; Tempest et al., 2015). This has resulted in the restoration of intertidal conditions, but not full restoration of the hydrological regime and the physical structure of the intertidal environment which may have consequences for the ecological functioning and ecosystem services provided. It has been proposed that the structural differences between MR and natural sites are the cause of water-logging and poor drainage, which have been attributed to poor saltmarsh species abundance and diversity within MR sites (e.g. Mossman et al., 2012). Clear differences in sediment structure for sites of different former land use were found at the Medmerry Managed Realignment Site. Therefore, it would be anticipated that sites with reduced porosity and pore connectivity would have lower subsurface flow, no or low concentrations of dissolved oxygen, and anoxic sediment. However, analyses of the geochemical profiles at Medmerry do not yet match this expectation.

Medmerry is still a developing site on the open coast and, therefore, has not experienced a large accretion of intertidal sediment on the former terrestrial land surface, such as observed in older MR sites found in sediment-rich estuarine environments (Spencer et al., 2017; Spencer et al., 2008; Watts et al., 2003; Wolanski and Elliott, 2016). It remains to be seen how the geochemical profiles develop following further accretion of sediment. However, without the accretion of sediment on top of the terrestrial horizon, tidal waters appear to have been able to drain through the terrestrial facies. An exception is the site of Core 2; in the second sample taken from this site sediment appeared black and anoxic, with evidence of water pooling at the terrestrial boundary and reduced hydrological connectivity through the contact between the facies. These findings suggest that hydrological and geochemical differences found in MR sites compared to natural saltmarshes are not caused

633 by sub-surface differences owing to the former land use, but by the formation of an
634 unconformity in the sediment column as a result of (a) the accretion of sediment, and (b)
635 sharp physicochemical contrasts between the accreted upper unit and the underlying
636 sediment. For the latter, in Core 2, it is likely that the formation of an anoxic unit has been
637 driven by the decay of terrestrial vegetation trapped and buried under the accreted
638 sediment following site inundation (French, 2006).

639

640 7 Conclusion

641

642 In this paper, differences in the sub-surface structure and physiochemical properties of
643 inundated sites with different former land use histories have been investigated at the
644 Medmerry Managed Realignment Site, during the initial 16 and 36 months after site
645 inundation. A novel combination of repeated broad- and intensive-scale analysis was used
646 to assess differences in the subsurface sediment structure and early geochemical evolution
647 in the three years following site inundation. Results indicate a number of new findings,
648 including:

649 • Clear differences are present in the sediment structure and properties at different
650 sites as a result of contrasts in the former land use. Broad-scale analysis suggests
651 sites formerly used more intensively for agricultural purposes have lower moisture
652 content and loss on ignition, with intensive-scale analysis suggesting pore networks
653 were more complex but were less connected and aligned at these sites.

- Evidence of reduced drainage and anoxic conditions, identified in previous studies (e.g. Spencer et al., 2017; Tempest et al., 2015) as a result of modifications caused by a site's terrestrial history, were not found at Medmerry except at the site which had experienced the highest level of accretion (*ca*. 7 cm in 36 months).

Further work is now required to assess if the differences in sediment structure, identified in this study, can be detected in other (including older) MR sites where greater levels of post-site inundation accumulation have occurred. The findings in this study indicate that the formation of an aquaclude, reducing vertical solute transfer between facies, is not a direct consequence of changes to the sediment caused by the former land use, but is the result of the accretion of sediment, coupled with sharp physicochemical contrasts between the accreted upper layer and the underlying sediment. Many MR sites are designed to accumulate sediment, but these findings highlight the need for improved awareness of sediment accretion in decision-making in the design of MR sites, alongside hydrodynamic and topographic considerations. While further work on other MR sites is needed to assess how widespread this accretionary effect is, the data presented here indicate that sites need to be designed to encourage rapid accumulation of intertidal sediment, burying the terrestrial boundary and so minimising the effect of an aquaclude. Alternatively, predictions need to be adjusted to anticipate reduced saltmarsh diversity abundance, and therefore ecosystem services delivery, until sufficient sediment has been accreted.

Acknowledgements

The authors would like to thank the two anonymous reviewers for their comments, which have helped improve the manuscript. The authors would also like to thank: Matthew Leake (University of Brighton) for his assistance during field work, Magda Grove, Peter Lyons (both University of Brighton) and Lucy Diggens (Queen Mary University of London) for their assistance with laboratory analysis, Callum Firth for his support and guidance during JD's studentship and during fieldwork. X-ray microtomography was carried out by the School of Geography, Queen Mary University of London. The authors are grateful to the BOSCORF facility at the National Oceanography Centre (Southampton) for access to Itrax facilities. Research was funded by the Environment Agency (United Kingdom).

References

Auxtero E, Shamshuddin J, Paramananthan S. Mineralogy, morphology and classification of acid sulfate soils in Pulau Lumut, Selangor. Pertanika 1991; 14: 43-51.

Bergen SD, Bolton SM, L. Fridley J. Design principles for ecological engineering. Ecological Engineering 2001; 18: 201-210.

Berrow ML, Stein WM. Extraction of metals from soils and sewage sludges by refluxing with aqua regia. Analyst 1983; 108: 277-285.

Beven K, Germann P. Macropores and water flow in soils revisited. Water Resources Research 2013; 49: 3071-3092.

Bone AE. The shaping of the Selsey coastline: a review of the geomorphology, archaeology and history. Tertiary Research 1996; 16: 5-14.

Burton ED, Bush RT, Johnston SG, Sullivan LA, Keene AF. Sulfur biogeochemical cycling and novel Fe-S mineralization pathways in a tidally re-flooded wetland. Geochimica Et Cosmochimica Acta 2011; 75: 3434-3451.

Cnudde V, Boone MN. High-resolution X-ray computed tomography in geosciences: A review of the current technology and applications. Earth-Science Reviews 2013; 123: 1-17.

Cochran JK, Hirschberg DJ, Wang J, Dere C. Atmospheric deposition of metals to coastal waters (Long Island Sound, New York USA): Evidence from saltmarsh deposits. Estuarine Coastal and Shelf Science 1998; 46: 503-522.

Cope S, Bradbury A, Gorczynska M. Solent Dynamic Coast Project: Main Report; A tool for SMP2, New Forest District Council/Channel Coastal Observatory, 2008.

Costanza R, d'Arge R, deGroot R, Farber S, Grasso M, Hannon B, et al. The value of the world's ecosystem services and natural capital. Nature 1997; 387: 253-260.

Crooks S, Pye K. Sedimentological controls on the erosion and morphology of saltmarshes: implications for flood defence and habitat recreation. In: Pye K, Allen JRL, editors. Coastal and Estuarine Environments: Sedimentology, Geomorphology and Geoarchaeology. 175, 2000, pp. 207-222.

Crooks S, Schutten J, Sheern GD, Pye K, Davy AJ. Drainage and elevation as factors in the restoration of salt marsh in Britain. Restoration Ecology 2002; 10: 591-602.

Croudace IW, Rindby A, Rothwell RG. ITRAX: description and evaluation of a new multi-function X-ray core scanner. Geological Society, London, Special Publications 2006; 267: 51-63.

Cundy AB, Croudace IW. Sedimentary and geochemical variations in a salt-marsh mud flat environment from the mesotidal Hamble estuary, southern England. Marine Chemistry 1995; 51: 115-132.

Cundy AB, Kortekaas S, Dewez T, Stewart IS, Collins PEF, Croudace IW, et al. Coastal wetlands as recorders of earthquake subsidence in the Aegean: a case study of the 1894 Gulf of Atalanti earthquakes, central Greece. Marine Geology 2000; 170: 3-26.

Cundy AB, Long AJ, Hill CT, Spencer C, Croudace IW. Sedimentary response of Pagham Harbour, southern England to barrier breaching in AD 1910. Geomorphology 2002; 46: 163-176.

Cundy AB, Sprague D, Hopkinson L, Maroukian H, Gaki-Papanastassiou K, Papanastassiou D, et al. Geochemical and stratigraphic indicators of late Holocene coastal evolution in the Gythio area, southern Peloponnese, Greece. Marine Geology 2006; 230: 161-177.

734 Dale J, Burgess HM, Burnside NG, Kilkie P, Nash DJ, Cundy AB. The evolution of embryonic
735 creek systems in a recently inundated large open coast managed realignment site.
736 Anthropocene Coasts 2018a; 1: 16-33.
737 Dale J, Burgess HM, Cundy AB. Sedimentation rhythms and hydrodynamics in two
738 engineered environments in an open coast managed realignment site. Marine
739 Geology 2017; 383: 120-131.
740 Dale J, Burgess HM, Nash DJ, Cundy AB. Hydrodynamics and sedimentary processes in the
741 main drainage channel of a large open coast managed realignment site. Estuarine,
742 Coastal and Shelf Science 2018b.
743 Davy AJ, Brown MJH, Mossman HL, Grant A. Colonization of a newly developing salt marsh:
744 disentangling independent effects of elevation and redox potential on halophytes.
745 Journal of Ecology 2011; 99: 1350-1357.
746 Doherty JM, Callaway JC, Zedler JB. Diversity-function relationships changed in a long-term
747 restoration experiment. Ecological Applications 2011; 21: 2143-2155.
748 Doody JP. 'Coastal squeeze' - an historical perspective. Journal of Coastal Conservation
749 2004; 10: 129-138.
750 Elliott M, Mander L, Mazik K, Simenstad C, Valesini F, Whitfield A, et al. Ecoengineering with
751 Ecohydrology: Successes and failures in estuarine restoration. Estuarine, Coastal and
752 Shelf Science 2016; 176: 12-35.
753 Environment Agency. Pagham to East Head Coastal Defence Strategy, Worthing, 2007.
754 Erfanzadeh R, Garbutt A, Petillon J, Maelfait JP, Hoffmann M. Factors affecting the success
755 of early salt-marsh colonizers: seed availability rather than site suitability and
756 dispersal traits. Plant Ecology 2010; 206: 335-347.
757 Esteves LS. Is managed realignment a sustainable long-term coastal management approach?
758 Journal of Coastal Research 2013; Special Issue 65: 933-938.
759 European Parliament and the Council of the European Commission. Council directive
760 92/43/EEC of 21 May 1992 on the conservation of natural habitats and of wild fauna
761 and flora. Official Journal of the European Communities 1992; Series L206:
762 22.12.2000.
763 Foster NM, Hudson MD, Bray S, Nicholls RJ. Research, policy and practice for the
764 conservation and sustainable use of intertidal mudflats and saltmarshes in the Solent
765 from 1800 to 2016. Environmental Science & Policy 2014; 38: 59-71.
766 French PW. Managed realignment - The developing story of a comparatively new approach
767 to soft engineering. Estuarine Coastal and Shelf Science 2006; 67: 409-423.
768 Hazelden J, Boorman LA. Soils and 'managed retreat' in South East England. Soil Use and
769 Management 2001; 17: 150-154.
770 Howe AJ, Rodriguez JF, Spencer J, MacFarlane GR, Saintilan N. Response of estuarine
771 wetlands to reinstatement of tidal flows. Marine and Freshwater Research 2010; 61:
772 702-713.
773 Hvorslev MJ. Subsurface exploration and sampling of soils for civil engineering purposes.
774 Vicksburg, Mississippi: Waterways Experiment Station, 1949.
775 Johnston SG, Keene AF, Bush RT, Burton ED, Sullivan LA, Isaacson L, et al. Iron geochemical
776 zonation in a tidally inundated acid sulfate soil wetland. Chemical Geology 2011;
777 280: 257-270.
778 Ketcham RA, Carlson WD. Acquisition, optimization and interpretation of X-ray computed
779 tomographic imagery: applications to the geosciences. Computers & Geosciences
780 2001; 27: 381-400.

781 Koretsky CM, Van Cappellen P, DiChristina TJ, Kostka JE, Lowe KL, Moore CM, et al. Salt
782 marsh pore water geochemistry does not correlate with microbial community
783 structure. Estuarine, Coastal and Shelf Science 2005; 62: 233-251.
784 Krawiec K. Medmerry, West Sussex, UK: Coastal Evolution from the Neolithic to the
785 Medieval Period and Community Resilience to Environmental Change. The Historic
786 Environment: Policy & Practice 2017; 8: 101-112.
787 Luther GW, Church TM. Seasonal cycling of sulfur and iron in porewaters of a Delaware salt-
788 marsh. Marine Chemistry 1988; 23: 295-309.
789 Marani M, Silvestri S, Belluco E, Ursino N, Comerlati A, Tosatto O, et al. Spatial organization
790 and ecohydrological interactions in oxygen-limited vegetation ecosystems. Water
791 Resources Research 2006; 42.
792 Mazik K, Musk W, Dawes O, Solyanko K, Brown S, Mander L, et al. Managed realignment as
793 compensation for the loss of intertidal mudflat: A short term solution to a long term
794 problem? Estuarine, Coastal and Shelf Science 2010; 90: 11-20.
795 Miller H, Croudace IW, Bull JM, Cotterill CJ, Dix JK, Taylor RN. A 500 Year Sediment Lake
796 Record of Anthropogenic and Natural Inputs to Windermere (English Lake District)
797 Using Double-Spike Lead Isotopes, Radiochronology, and Sediment Microanalysis.
798 Environmental Science & Technology 2014; 48: 7254-7263.
799 Moller I, Kudella M, Rupprecht F, Spencer T, Paul M, van Wesenbeeck BK, et al. Wave
800 attenuation over coastal salt marshes under storm surge conditions. Nature
801 Geoscience 2014; 7: 727-731.
802 Mossman HL, Brown MJH, Davy AJ, Grant A. Constraints on Salt Marsh Development
803 Following Managed Coastal Realignment: Dispersal Limitation or Environmental
804 Tolerance? Restoration Ecology 2012; 20: 65-75.
805 Odgaard A. Three-dimensional methods for quantification of cancellous bone architecture.
806 Bone 1997; 20: 315-328.
807 Pearce J, Khan S, Lewis P. Medmerry managed realignment–sustainable coastal
808 management to gain multiple benefits. ICE Coastal Management. Innovative Coastal
809 Zone Management: Sustainable Engineering for a Dynamic Coast., Belfast, UK, 2011.
810 Polder G, Hovens H, Zweers A. Measuring shoot length of submerged aquatic plants using
811 graph analysis. Proceedings of the ImageJ User and Developer Conference 2010,
812 Mondorf-les-Bains, Luxembourg, 27-29 October 2010, 2010, pp. 172-177.
813 Reid MK, Spencer KL. Use of principal components analysis (PCA) on estuarine sediment
814 datasets: The effect of data pre-treatment. Environmental Pollution 2009; 157:
815 2275-2281.
816 Rowell DL. Soil science: Methods & applications. Harlow, Essex: Longman Scientific &
817 Technical, 1994.
818 Rupprecht F, Moller I, Paul M, Kudella M, Spencer T, van Wesenbeeck BK, et al. Vegetation-
819 wave interactions in salt marshes under storm surge conditions. Ecological
820 Engineering 2017; 100: 301-315.
821 Shennan I, Long AJ, Rutherford MM, Green FM, Innes JB, Lloyd JM, et al. Tidal marsh
822 stratigraphy, sea-level change and large earthquakes, i: a 5000 year record in
823 washington, U.S.A. Quaternary Science Reviews 1996; 15: 1023-1059.
824 Shennan I, Long AJ, Rutherford MM, Innes JB, Green FM, Walker KJ. Tidal marsh
825 stratigraphy, sea-level change and large earthquakes—ii: Submergence events
826 during the last 3500 years at Netarts Bay, Oregon, USA. Quaternary Science Reviews
827 1998; 17: 365-393.

828 Spencer KL, Carr SJ, Diggens LM, Tempest JA, Morris MA, Harvey GL. The impact of pre-
829 restoration land-use and disturbance on sediment structure, hydrology and the
830 sediment geochemical environment in restored saltmarshes. Science of The Total
831 Environment 2017; 587–588: 47-58.
832 Spencer KL, Cundy AB, Croudace IW. Heavy metal distribution and early-diagenesis in salt
833 marsh sediments from the Medway Estuary, Kent, UK. Estuarine Coastal and Shelf
834 Science 2003; 57: 43-54.
835 Spencer KL, Cundy AB, Davies-Hearn S, Hughes R, Turner S, MacLeod CL. Physicochemical
836 changes in sediments at Orplands Farm, Essex, UK following 8 years of managed
837 realignment. Estuarine Coastal and Shelf Science 2008; 76: 608-619.
838 Tempest JA, Harvey GL, Spencer KL. Modified sediments and subsurface hydrology in natural
839 and recreated salt marshes and implications for delivery of ecosystem services.
840 Hydrological Processes 2015; 29: 2346-2357.
841 Violante A, Barberis E, Pigna M, Boero V. Factors affecting the formation, nature, and
842 properties of iron precipitation products at the soil-root interface. Journal of Plant
843 Nutrition 2003; 26: 1889-1908.
844 Vogel HJ. Morphological determination of pore connectivity as a function of pore size using
845 serial sections. European Journal of Soil Science 1997; 48: 365-377.
846 Vranken M, Oenema O, Mulder J. Effects of tide range alterations on salt-marsh sediments
847 in the eastern Scheldt, SW Netherlands. Hydrobiologia 1990; 195: 13-20.
848 Watts CW, Tolhurst TJ, Black KS, Whitmore AP. In situ measurements of erosion shear stress
849 and geotechnical shear strength of the intertidal sediments of the experimental
850 managed realignment scheme at Tollesbury, Essex, UK. Estuarine Coastal and Shelf
851 Science 2003; 58: 611-620.
852 Wilson AM, Evans T, Moore W, Schutte CA, Joye SB, Hughes AH, et al. Groundwater controls
853 ecological zonation of salt marsh macrophytes. Ecology 2015; 96: 840-849.
854 Wolanski E, Elliott M. Estuarine Ecohydrology (Second Edition). Boston: Elsevier, 2016.
855 Zwolsman JJG, Berger GW, Vaneck GTM. Sediment accumulation rates, historical input,
856 postdepositional mobility and retention of major elements and trace-metals in salt-
857 marsh sediments of the Scheldt estuary, SW Netherlands. Marine Chemistry 1993;
858 44: 73-94.

859

860

861

<table>
<tr><th colspan="2">Medmerry Managed Realignment Site (West Sussex, United Kingdom)</th><th>Orplands Farm Managed Realignment Site (Essex, United Kingdom)</th><th>Natural Saltmarsh (Hamble estuary, Hampshire, United Kingdom)</th></tr>
<tr><td>Post-site inundation intertidal</td><td rowspan="3">Physical properties varied in terrestrial unit but mottled oxic conditions were found throughout suggesting a variable water table and that vertical solute transfer is not inhibited</td><td>Post-site inundation: Poorly consolidated oxic unit with a high abundant root material and omplex, interconnected pore networks</td><td>Layer 1: Thin (mm) oxidised surface layer rich in plant litter</td></tr>
<tr><td>Terrestrial</td><td rowspan="2">Terrestrial: Firmer sediment layer, lower in organic and moisture content. Geochemical (lower Fe and Mn concentrations), structural (reduced pore distribution and complexity) and hydrological (reduced vertical water flux) evidences suggests reduced solute transfer between units</td><td>Layer 2: Mottled oxic zone with evidence of a fluctuating water table, rich in abundant (living) root material</td></tr>
<tr><td>Pre-reclamation intertidal</td><td>Layer 3: Black unit with reducing anoxic conditions, increased water content</td></tr>
</table>

Graphical Abstract: Schematic comparison of the sub-surface physicochemical properties of the sediment found at the Medmerry Managed Realignment Site (this study), Orplands Farm Managed Realignment Site, U.K. (Spencer et al., 2008; Tempest et al., 2015; Spencer et al., 2017) and a typical natural minerogenic saltmarsh (Cundy and Croudace, 1995). Not drawn to uniform vertical scale.

Figures

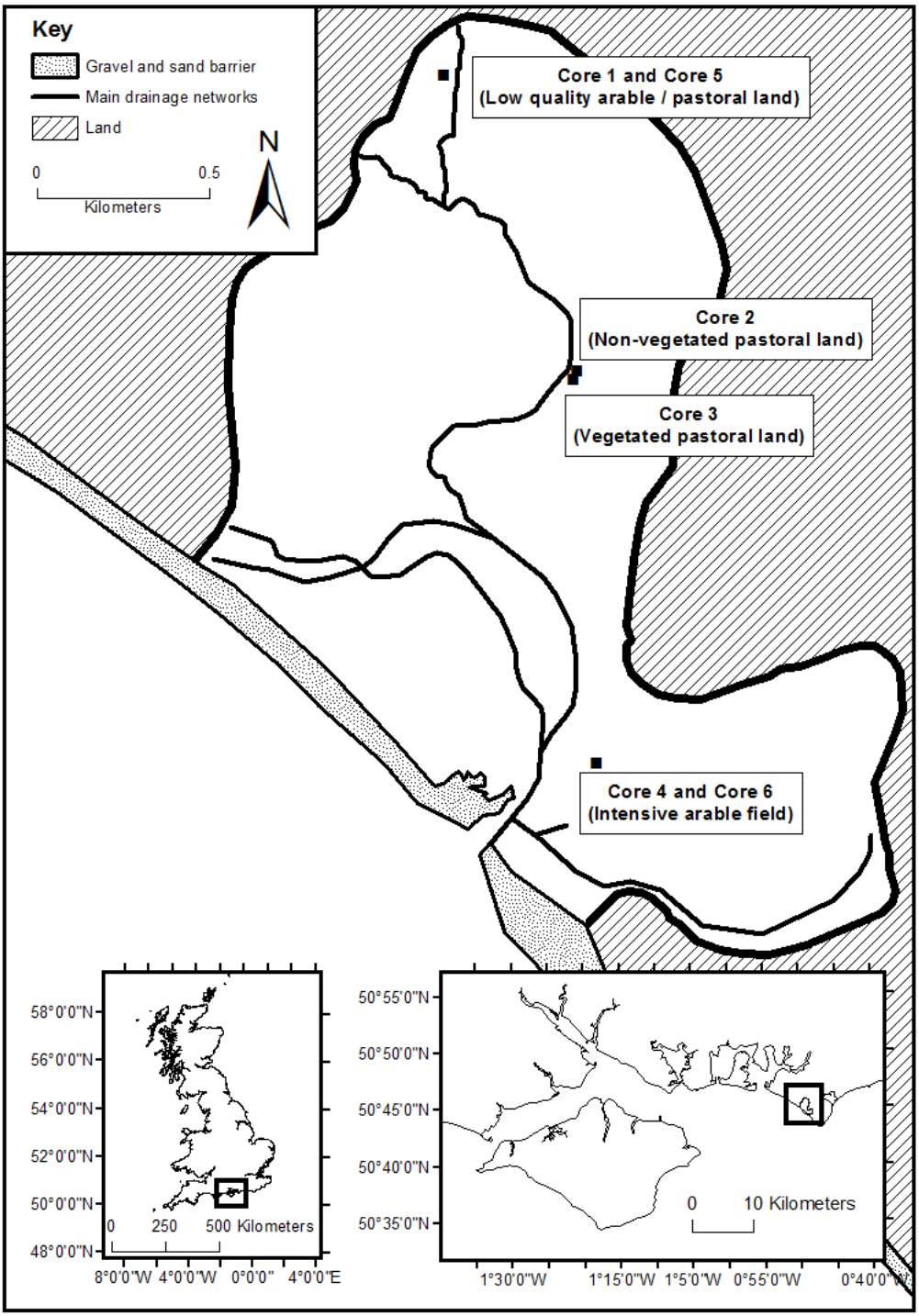

Figure 1: The Medmerry Managed Realignment Site (West Sussex, UK) and wider national (insert, left) and regional (insert, right) location. Coring locations are named and marked with black squares.

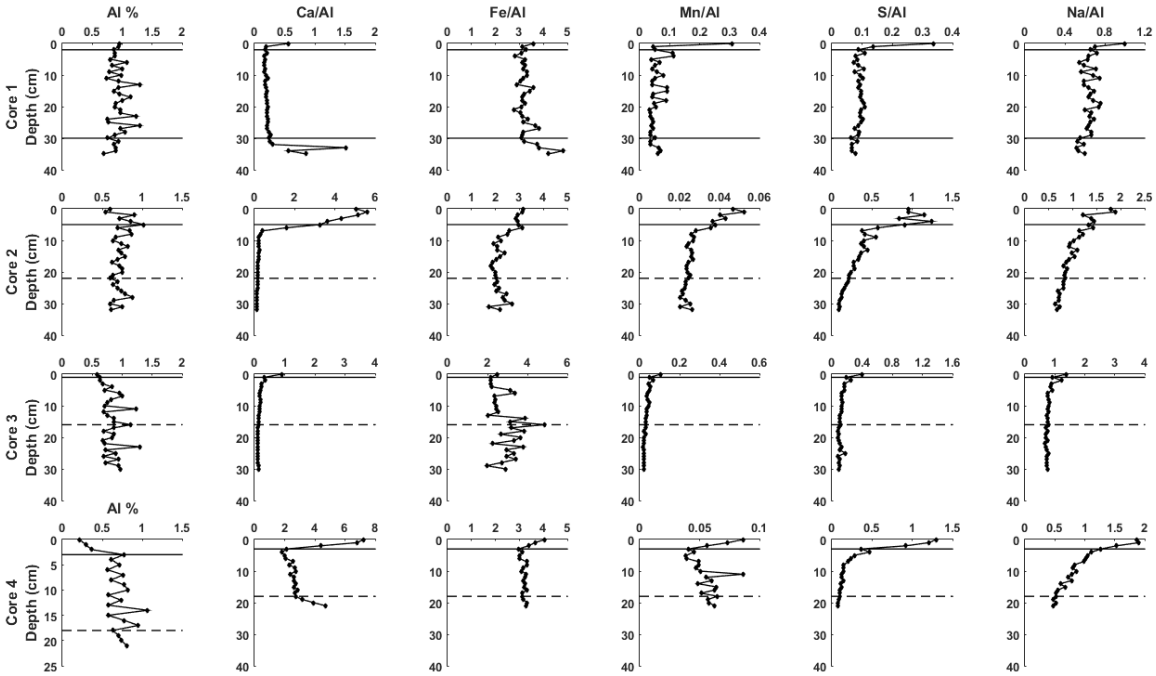

Figure 2: Variations in Al, Ca, Fe, Mn, S and Na concentration with depth from the 2015 core samples.

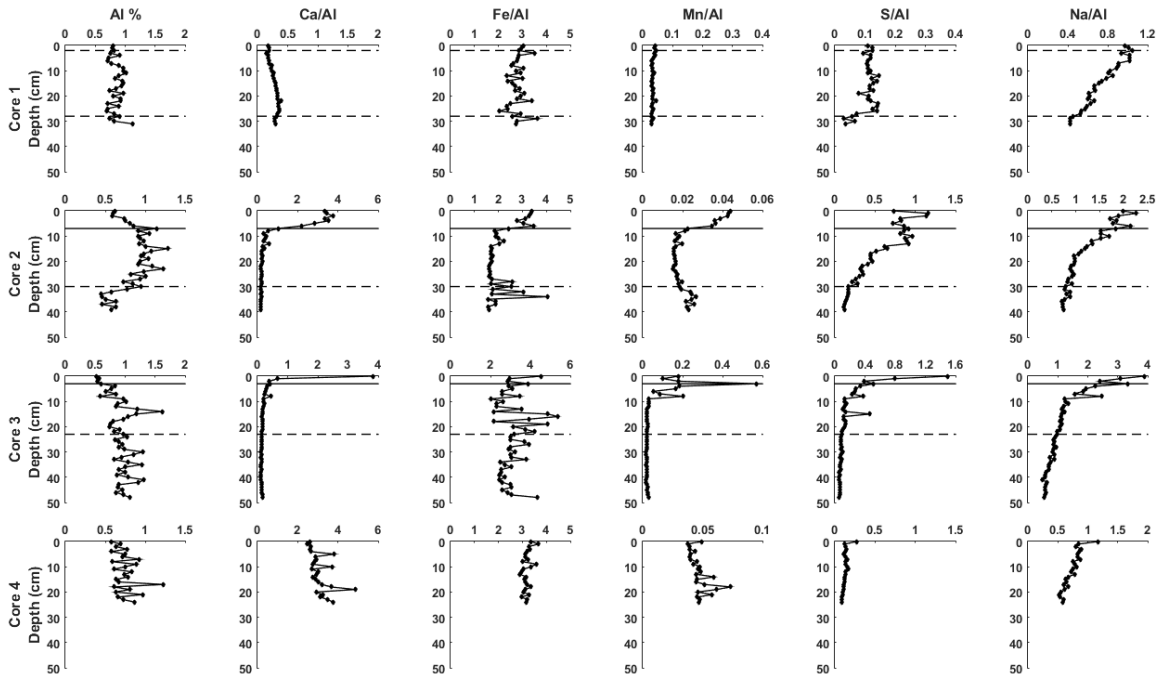

Figure 3: Variations in Al, Ca, Fe, Mn, S and Na concentration with depth from the 2016 core samples.

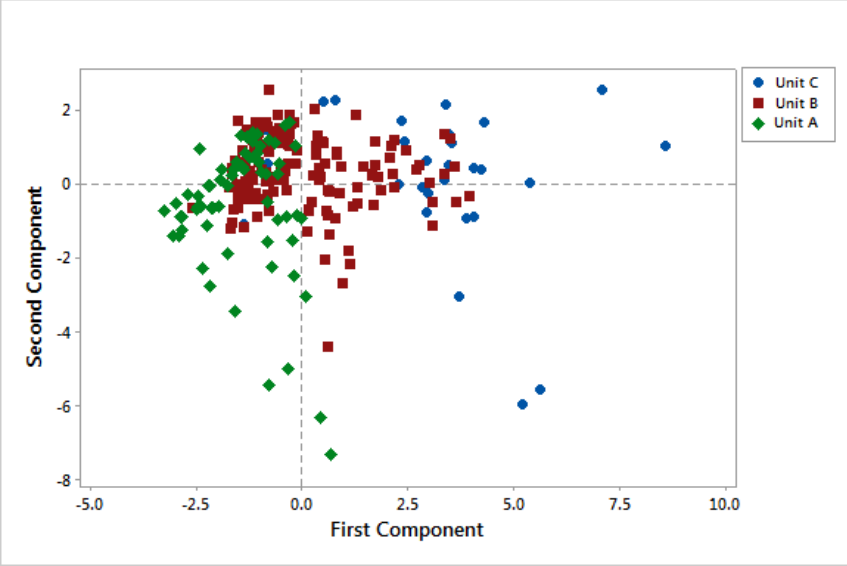

Figure 4: Principle component analysis (PCA) scores for the three sediment units identified in Cores 1 – 4 in 2015 and Cores 1 – 3 in 2016. Components 1 and 2 collectively accounted for 49.6 % of the total variance.

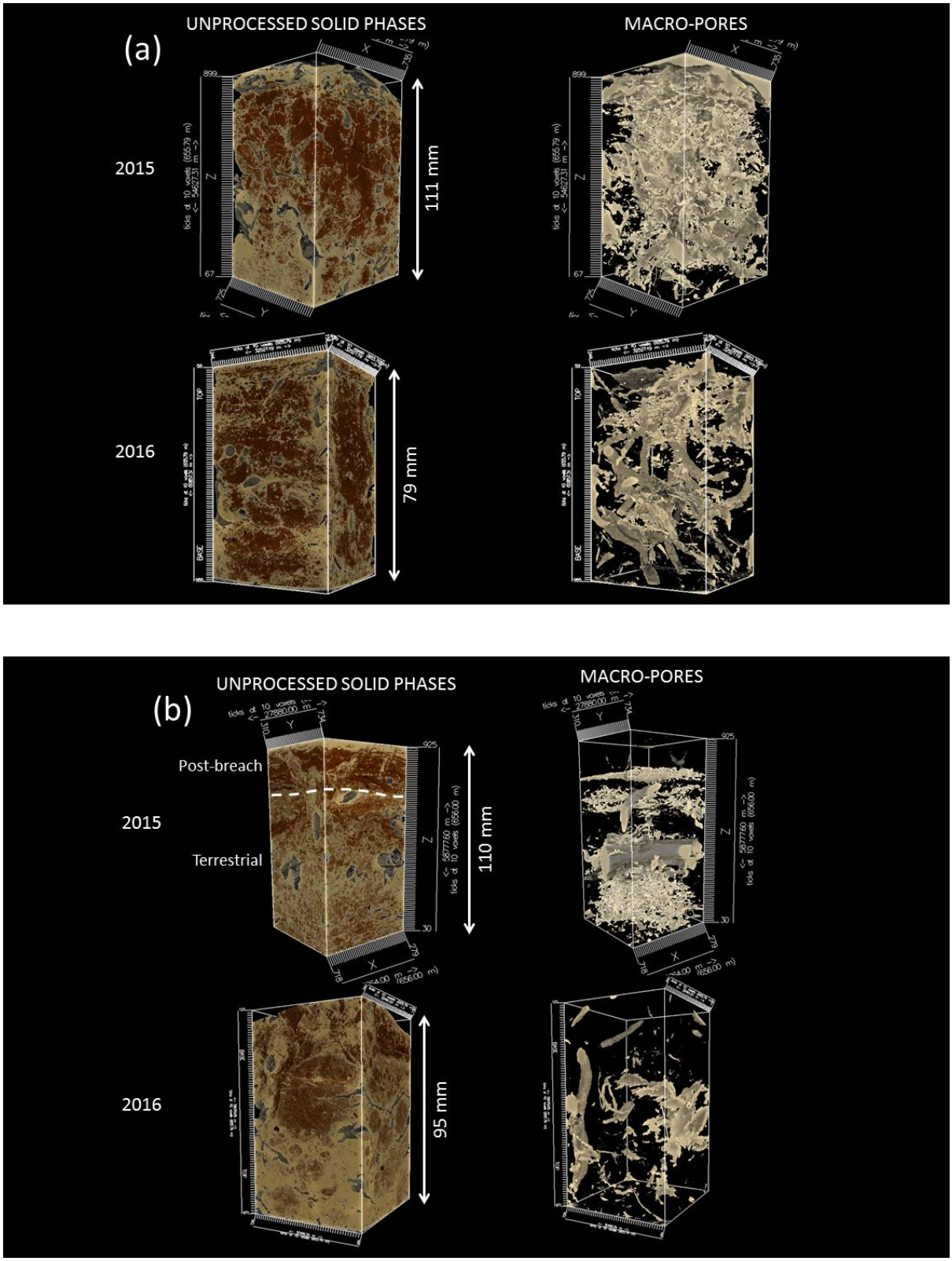

Figure 5: Reconstructions of sediment phases imaged used µCT analysis in (a) Core 1 and (b) Core 2.

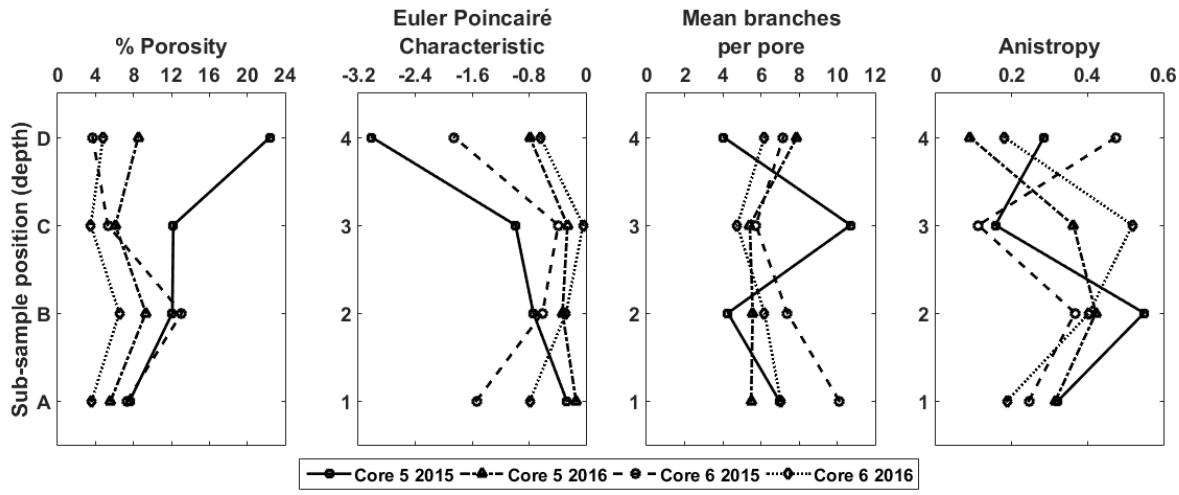

Figure 6: Porosity characteristics for sub-samples of Cores 5 and 6 in 2016 and 2017.

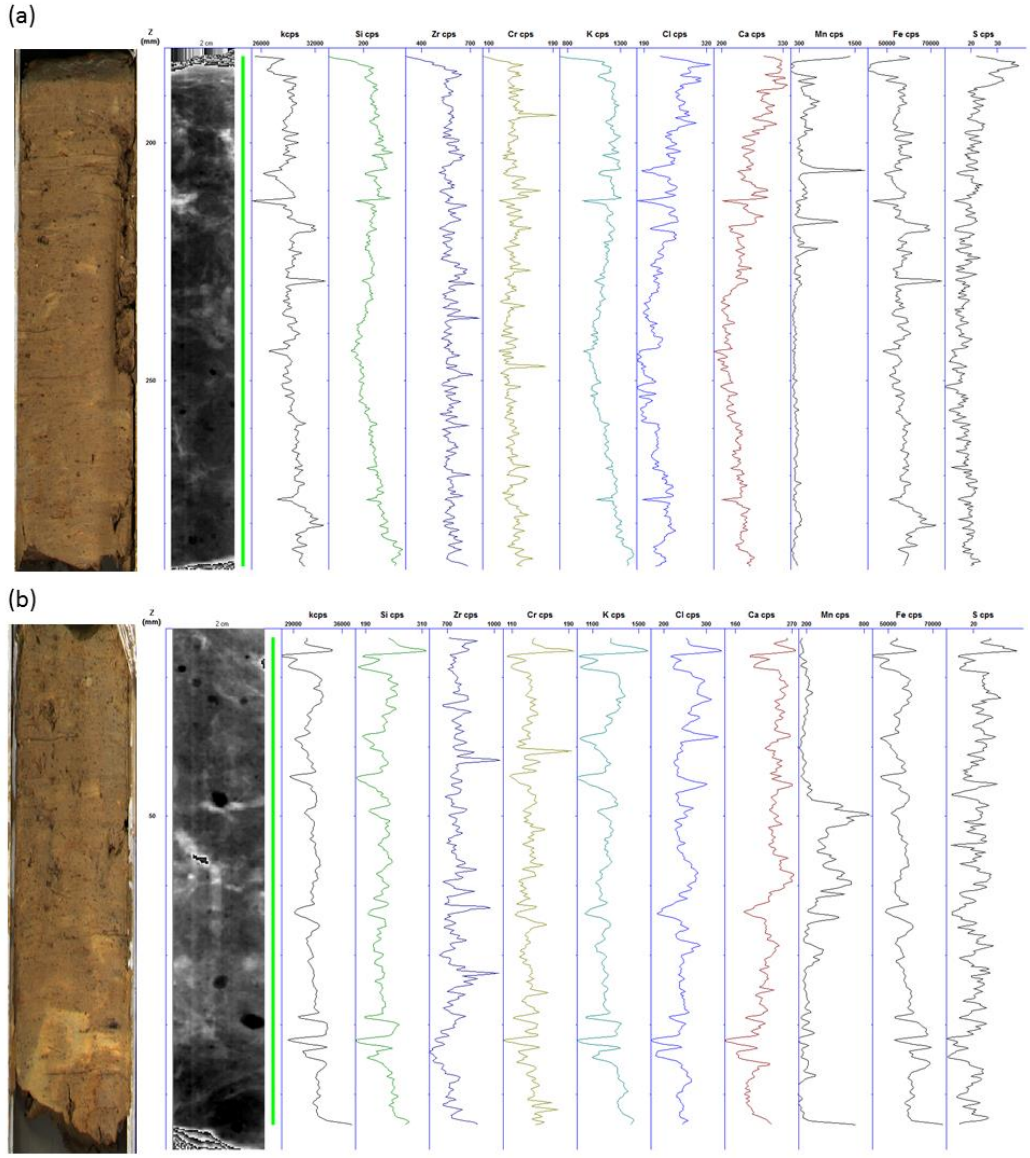

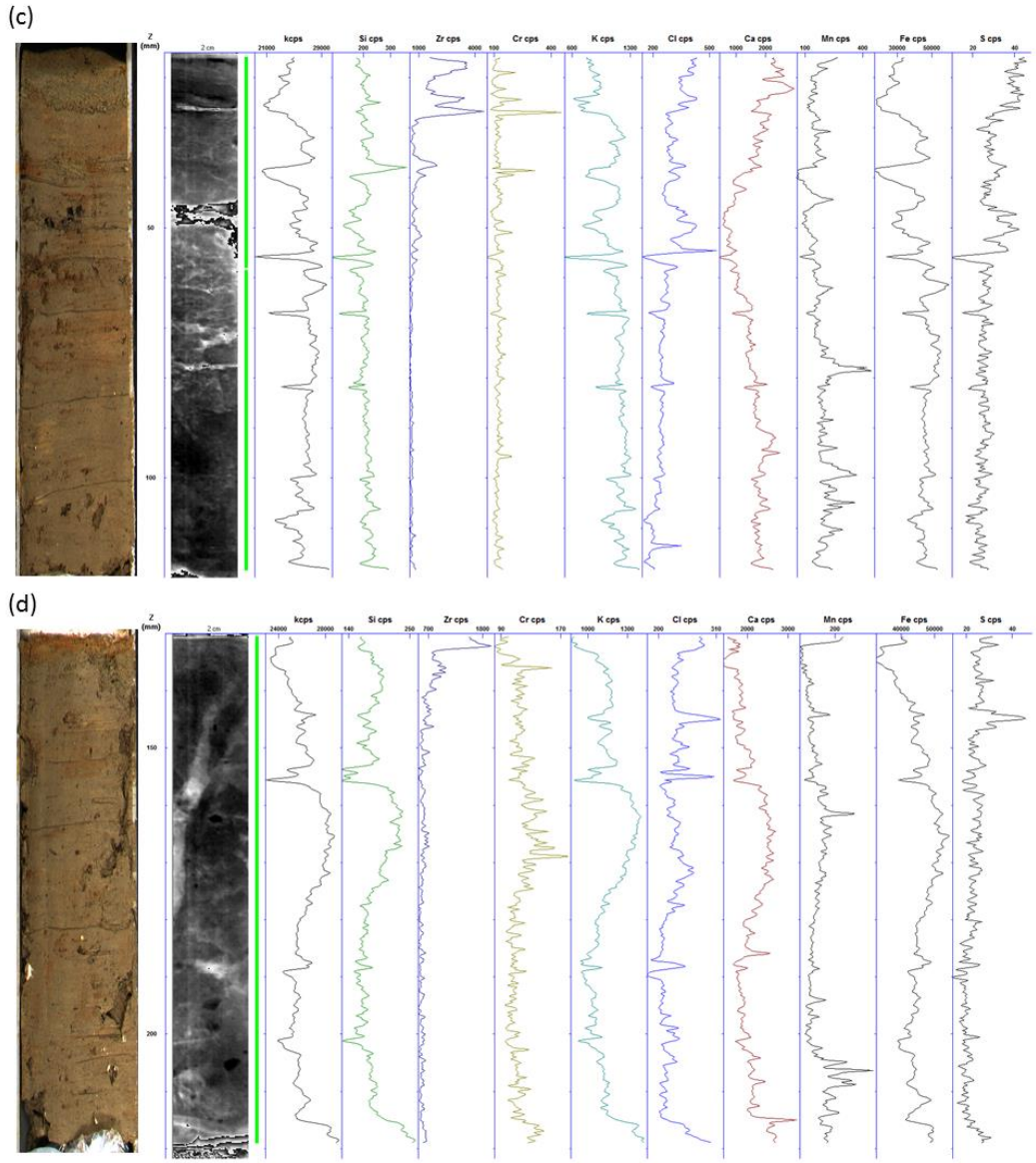

Figure 7: Si, Zr, Cr, K, Cl, Ca, Mn, Fe and S distribution, X-radiograph and photograph of core from (a) Core 5_{15}, (b) Core 5_{16}, (c) Core 6_{15} and (d) Core 6_{16}. Data are from Itrax scanning: X-axis shows X-ray response, y-axis represents depth.

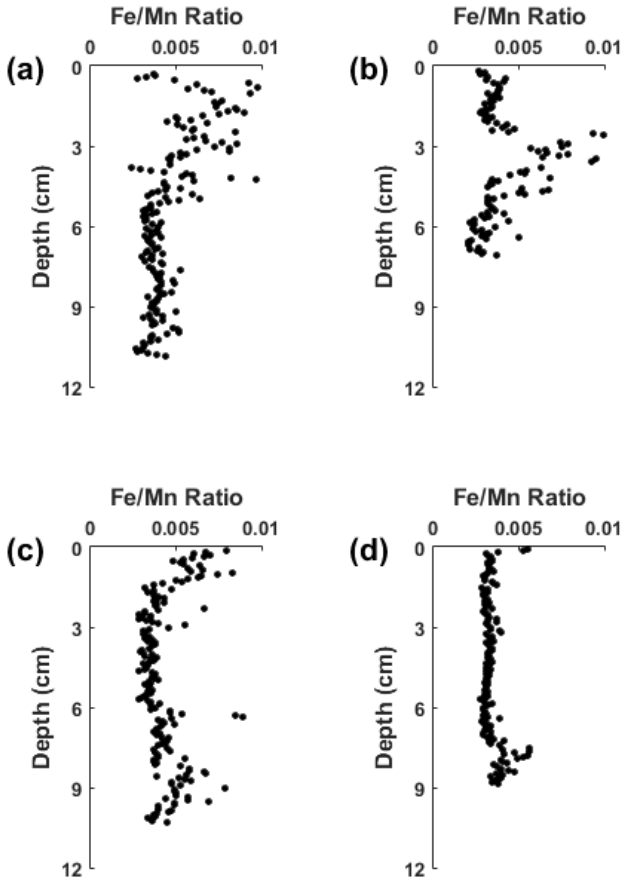

Figure 8: Fe / Mn ratio for (a) Core 5_{15}, (b) Core 5_{16}, (c) Core 6_{15} and (d) Core 6_{16} derived from Itrax geochemical data.

Tables

Table 1: Former (terrestrial) land use at sampling locations within the Medmerry Managed Realignment Site and the proposed structural state.

Site	Terrestrial Land Use	Proposed Structure and Composition
Core 1	Low quality arable / pastoral land	Some compaction but interconnected pore networks still expected to be present
Core 2	Non-vegetated pastoral land	Uncompact freely draining sediment
Core 3	Vegetated pastoral land	
Core 4	Intensive arable field	Compact, with low abundance of pore networks resulting lower subsurface solute transfer and anoxic conditions

Table 2: Mean values for physical sediment characteristics for the three sediment units identified (see text for discussion) at the four coring sites (see Figure 1 for locations) in 2015 and 2016.

			Wet Bulk Density ($kg\ m^{-3}$)		Moisture Content (%)		Porosity		Loss on Ignition (%)		Median Grain Size (µm)		Mud (clay + silt) Content (%)	
			Mean	SD	Mean	SD	Mean	SD	Mean	SD	Mean	SD	Mean	SD
Core 1	2015	Unit C	0.76	0.2	62.22	22.14	0.68	0.11	7.58	0.59	6.58	0.58	97.41	0.68
		Unit B	0.86	0.16	49.04	3.59	0.62	0.07	6.95	2.9	8.44	1.58	94.12	2.52
		Unit A	0.89	0.16	43.99	9.05	0.58	0.09	7.51	2.16	15.34	3.76	92.23	2.95
	2016	Unit C	1.94	0.34	44.82	0.78	0.5	0.09	6.79	11.33	6.03	1.88	89.83	9.77
		Unit B	1.88	0.22	46.42	3.49	0.52	0.06	6.16	5.49	6.71	1.05	87.28	5.25
		Unit A	2.08	0.35	41.84	4.86	0.44	0.11	4.07	3.74	6.19	0.41	91.2	1.45
Core 2	2015	Unit C	0.92	0.23	123.08	14.49	0.72	0.07	5.73	1.83	7.47	0.4	97.67	2.26
		Unit B	1.02	0.38	96.23	21.28	0.65	0.13	9.92	5.87	15.68	8.61	81.44	11.15
		Unit A	1.51	0.45	48.8	6.2	0.33	0.19	7.01	4.72	16.91	5.65	79.48	7.83
	2016	Unit C	1.48	0.27	100.92	5.59	0.72	0.05	4.96	6.15	10.05	2.04	77.36	6.76
		Unit B	1.39	0.33	97.37	29.84	0.73	0.09	12.48	8.54	11.51	7.96	68.23	9.39
		Unit A	1.75	0.3	40.69	8.3	0.53	0.1	4.83	11.1	33.15	25.68	54.1	14.62
Core 3	2015	Unit C	0.64	0.06	122.21	9.46	0.81	0.02	18.61	0.47	6.42	0.78	96.19	3.32
		Unit B	0.99	0.28	69.34	11.05	0.61	0.12	13.48	2.77	6.7	0.77	95.18	2.62
		Unit A	0.93	0.2	51.46	12.19	0.58	0.1	4.52	3.74	5.46	0.59	96.79	5.63
	2016	Unit C	1.39	0.21	118.04	26.02	0.76	0.03	19.21	3.65	11.06	0.86	73.86	3.16
		Unit B	1.71	0.28	69.06	17.39	0.61	0.09	9.88	6.89	7.46	2.46	84.49	7.96
		Unit A	2.18	0.28	40.66	3.64	0.41	0.08	3.24	8.7	7.39	3.25	84.81	9.4
Core 4	2015	Unit C	0.94	0.14	47.95	0.67	0.58	0.07	5.5	15.66	46.48	28.77	59.17	20.19
		Unit B	0.98	0.2	42.25	3.7	0.54	0.1	5.18	3.83	8.54	1.48	89.73	5.13
		Unit A	0.93	0.14	36.89	1.97	0.55	0.07	4.38	1.44	7.52	0.6	92.29	2.33
	2016		1.94	0.33	36.62	4.4	0.46	0.09	4.85	8.59	10.2	8.43	78.06	9.93

Table 3: Porosity analysis derived from µCT analysis divided into sub-samples. Data are presented based on different sediment facies. Core 5 was taken from an area of former lower intensity arable agriculture; Core 6 was taken from an area of former high intensity arable agriculture.

	% Macroporosity	Macro-pore abundance	Pore Connectivity (Euler-Poincairé Characteristic)	Pore network complexity (no. of braches per pore)	Pore Anisotropy
Core 5 2015 A-D	7.6 – 22.4	Low (mean 3672), particularly in the upper sub-sample	-3.01 – -0.27, increasing upwards apart from upper sub-sample	4.05 – 10.71 with no distinctive patterns evident	Moderately high (mean 0.33), although much higher in lower (A and B) sub-samples
Core 5 2016 A-D	5.6 – 6.1	High (mean 5265) although lower in the upper sub-sample	-0.79 – -0.14, increasing upwards apart from upper sub-sample	5.42 – 7.89. Higher in upper sub-sample compared to other three	Moderately high (mean 0.3), but particularly low in upper sub-sample
Core 6 2015 lower facies A-C	5.3 – 13.1	High (mean 5133) and decreasing with depth	-1.54 – 0.39, increasing upwards apart from upper sub-sample	5.74 – 10.11, decreasing upwards.	Moderately low (mean 0.24)
Core 6 2015 upper facies D (post-breach)	3.7	Very high (9458)	-1.85	7.17, greater than the preceding sub-sample	High (0.48)
Core 6 2016 A-D	3.5 – 6.5	Moderately high (mean 4608) and decreasing downwards	-0.79 – -0.04, increasing upwards apart from upper sub-sample	4.76 – 7.04, following same pattern as 2015 sample.	Moderately high (mean 0.32), although lower in upper and lower sub-samples (A and D)